International Journal of Basic and Applied Sciences, 14 (2) (2025) 634-644

International Journal of Basic and Applied Sciences

Website: www.sciencepubco.com/index.php/IJBAS
https://doi.org/10.14419/fwq0t273
Research paper

Assessments of Rock Fall and Joint Failure Risk in A Geologically Complex Section, South Cut 8 Area, DK2 Jwaneng Pit, Botswana

Morwaake Brian Ntehelang *, Rahul Verma, Yendaw, Jerome Anabannye

Department of Mineral Resources, Botswana International University of Science & Technology
**Corresponding author E-mail: vermar@biust.ac.bw*

Received: May 26, 2025, Accepted: June 5, 2025, Published: July 6, 2025

Abstract

Jwaneng Mine is one of the richest diamond mines in the world. This mine is the flagship of Debswana due to the substantially higher dollar per carat obtained for its gems. Jwaneng Mine contributes about 60-70% of Debswana's total revenue. Currently, Jwaneng is mining at a depth of 452 metres and is expected to reach 816 metres by 2034. The Jwaneng kimberlites are emplaced in a thick sequence of shales, sandstones, and dolomites of the Kalahari Formation, with thin occurrences of mudstones and siltstones in areas. The Jwaneng Mine exploits a diamond-bearing Kimberlite complex of three main pipes known as the DK2 Kimberlite. The mine is currently being expanded through the Cut 9 underground project. The deepening and widening of the pit have introduced complicated geotechnical issues, particularly on the southern side of the excavation. The steep rock slopes and the presence of primary & secondary discontinuities, such as joints, bedding planes, and faults, heighten the risk of rockfall and structural failure, are significant threat to personnel safety, operational efficiency, and equipment integrity. The present work aims at a thorough and focused study of the evaluation of potential rock failure modes in the Cut 8 South region and for developing effective monitoring and mitigation strategies to ensure safe mining operations. Data obtained through geological and structural mapping of the Cut 8 South side was used to identify key discontinuities, including joint sets, faults, and bedding planes. Kinematic analysis using stereographic projection was done to assess potential failure modes such as planar, wedge, and toppling failures. Further, slope stability modelling was done to simulate potential failure scenarios under existing conditions. Both DIPS and RS2 confirm that the wedge failures were common in areas with high joint density. Controlled blasting methods were recommended to reduce the effects of vibration on joined rock masses. Another recommendation is the slope reinforcement through structural support via the targeted placement of shotcrete, wire mesh, and rock bolts in high-risk areas. Lastly the efficient water management is necessary to regulate pore pressures. Draining out thorough dewatering wells and horizontal drains must be set up.

Keywords: *Cut 8; Joints; DIPS; RS2; Slope Reinforcement; Dewatering.*

1. Introduction

Rockfall cases are common at the global level. [1] have expressed that estimation of rockfall hazards is usually based only on hazards related to rockfall propagation. The rockfall failure hazard is not currently well defined, and only a few studies have truly addressed this topic. They have advocated high-resolution topography in real 3D, topography analysis and standard kinematic tests. [2] have used a high-precision and high-resolution digital terrain model (DTM), generated based on the point cloud data obtained by terrestrial laser scanning (TLS). The same has been used for rockfall simulation and automatic identification of structural planes.
[3] proposed a physically based deterministic model designed to accurately quantify rockfall hazards at a large scale. The model accounts for multiple rockfall failure modes and incorporates the key physical and structural parameters of the rock mass. Rockfall hazard is defined as the product of three factors: the rockfall failure probability, the probability of reaching a specific position, and the corresponding impact intensity. [4] presented a case study of Lotru Valley and Olt Gorge, Romania. He strictly linked the rockfall hazards to the two main causes: climatic and human activities, which created slope instability.
Jwaneng Mine is one of the richest diamond mines in the world. The mine became fully operational in August 1982, when it was officially opened by the then President of Botswana, His Excellency Sir Ketumile Masire. Construction of the mine and the township commenced rapidly, the former coming into full production in July 1982. Jwaneng Mine is the flagship of Debswana due to the substantially higher dollar per carat obtained for its gems. Jwaneng Mine contributes about 60-70% of Debswana's total revenue. Currently, Jwaneng is mining at a depth of 452 metres and is expected to reach 816 metres by 2034. The resource consists of three separate volcanic pipes/vents, namely: north, south, and center pipes (two additional small kimberlite bodies have also been intersected within the pit). The pipes erupted through Transvaal strata and the overlying Karoo sediments ~245 million years ago [5]. The location of the Jwaneng mine is shown in Fig.1. The aerial view of the Jwaneng mine is shown in Fig.2.

Fig. 1: Location of Jwaneng Town.

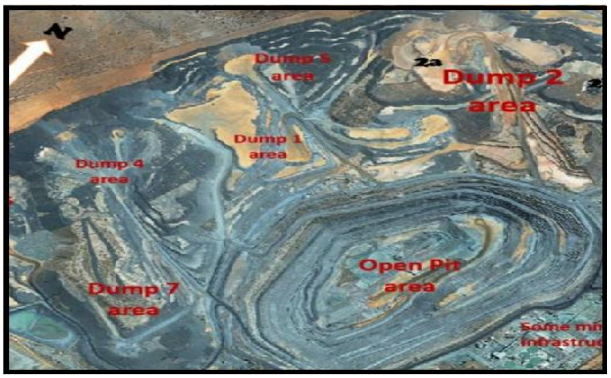

Fig. 2: Aerial View of the Jwaneng Mine Area.

2. Geology

The Jwaneng kimberlites are emplaced in a thick sequence of shales, sandstones, and dolomites with thin occurrences of mudstones and siltstones in areas as described by [6]. The Jwaneng Mine exploits a diamond-bearing Kimberlite complex of three main pipes known as the DK2 Kimberlite. The three main pipes have been named South (S), Centre (C), and North (N) pipes as illustrated in Figure 3. At the current levels of mining, the three main DK2 pipes have separated and appear as three separate pipes.

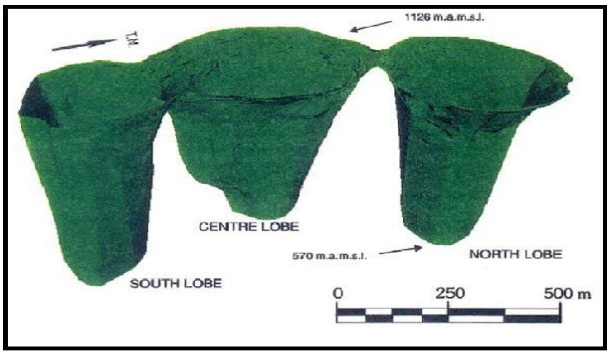

Fig. 3: Kimberlite Pipes in the DK2 Pit.

The three kimberlite pipes display geological inhomogeneity in terms of their modal composition and texture because of different genetic characteristics. The Jwaneng pipes are dominated by two contrasting textural types of kimberlites, which are the volcaniclastic kimberlite (VK) and the dark pyroclastic kimberlite (PK). The pyroclastic kimberlites occur only in the North pipe, with minor magmatic kimberlite [6].
The order of the lithology of the Jwaneng pit is presented in Table 1.

Table 1: Order of the Lithological Sequence of the Jwaneng Pit

Stratigraphic Name	Rock Type (Mine Rock Code)	Typical Thickness (M)
Kalahari Sequence	Sand and Calcrete (CS)	55-60
Upper Timeball Hill Formation	Laminated Shale (LS)	Residual
Lower Timeball Hill Formation	Carbonaceous Shale (CS)	30
Upper Rooighoogte Formation	Quartzite Shale (QS)	135
Chert Pebble Conglomerate	Bevets	0-4
Middle Rooighoogte Formation	Quartzite Shale (QS)	375
Lower Rooighoogte Formation	Carbonaceous Shale (CS)	10
Malmani Subgroup	Dolomite (DM)	Residual

3. Statement of the problem

The Jwaneng Debswana Mine is currently being expanded through the Cut 9 and underground projects. The deepening and widening of the pit have introduced complicated geotechnical issues, particularly on the southern side of the excavation. The steep rock slopes and the presence of discontinuities, such as joints, bedding planes, and faults, heighten the risk of rockfall and structural failure, posing are significant threat to personnel safety, operational efficiency, and equipment integrity. The present work aims at a thorough and focused study of the evaluation of potential rock failure modes in the Cut 8 South region. Gaining insight into these failure mechanisms is crucial for developing effective monitoring and mitigation strategies to ensure safe mining operations.
Objectives of the research

- To conduct detailed geological and structural mapping of the Cut 8 South side to identify key discontinuities, including joint sets, faults, and bedding planes.
- To perform kinematic analysis using stereographic projection methods to assess potential failure modes such as planar, wedge, and toppling failures.
- To use slope stability modelling tools to simulate potential failure scenarios under existing conditions.

4. Methodology

To evaluate the hazards of rockfall and joint-related failure in the Cut 8 South part of the Jwaneng Debswana Mine, the methodology is divided into two components:

a) Geotechnical investigative methodologies in the field
b) Geological investigative methodologies in the field
c) Analytical modelling through RocScience tool

a) Geotechnical investigative methodologies in the field

i) Drillholes placed strategically throughout the Cut 8 South region were geotechnically core-logged in the first phase. These core logs were analyzed with an emphasis on the structural characteristics of discontinuities.
ii) To identify and categorize lithological units, weathering properties, and fracture densities, core samples were inspected both mechanically and visually. The logging method's main goal was to thoroughly characterize discontinuities, which are essential for figuring out the rock mass's failure behaviour and structural integrity. The field investigations were conducted with a focus on orientation, spacing, aperture, persistence, surface roughness, infilling material, and moisture conditions; every discontinuity found within the core was noted. Alpha and beta angle measurements along the core axis were used to record orientation data, which were then reoriented using borehole deviation data to ascertain the true dip and dip direction.
iii) Features of the joints, such as smoothness, aperture, and waviness, were measured with calipers and classified by ISRM criteria.
iv) Infilling materials like clay, calcite, or gouge have a significant impact on shear strength; their existence was also noted.
v) To assess how water can lessen effective stress and perhaps promote failure, moisture conditions along discontinuities were observed.

b) Geological investigative methodologies in the field

i) The structural mapping done on exposed pit walls was combined with the core logging data to guarantee a three-dimensional understanding of the rock mass fabric.
ii) Joint sets, fault zones, bedding planes, and other planar features were measured as part of this mapping using a combination of digital mapping techniques and conventional geological equipment.
iii) Land LiDAR scanning and aerial drone photogrammetry were used in regions that were inaccessible because of steep slopes or safety concerns.
iv) To verify joint orientations and track continuity across the slope face, these techniques produced 3D terrain models and high-resolution georeferenced imagery.

c)Analytical modelling through the RocScience tool

i) Kinematic analysis was performed by processing the joint orientation data from both core logging and field mapping using stereographic projection techniques. This made it possible to identify several possible failure types, including toppling, wedge failure, and planar slide.
ii) To identify which failure mechanisms were most likely under the current geometric and structural parameters, as well as whether the direction of discontinuities was compatible with the slope face, a stereo net was created using specialized software (Dips).
iii) The next crucial phase in the process was numerical modelling. Stability simulations were conducted using geotechnical software, such as RocScience 2, to model a 2D slope, using input parameters obtained from the core logging and classification data. Slope geometry, joint patterns, rock strength, and outside variables like blasting vibrations and groundwater presence were all taken into consideration in the simulations.
iv) Finally, the risk interpretation was done, based on the above steps.

5. Data collection

- Field Data:

Scanline mapping was conducted along accessible pit walls and benches to directly measure discontinuity characteristics in situ. A scanline—a straight line of fixed orientation—was established on exposed rock faces, along which all intersecting joints were recorded systematically. The orientation of the scanline was selected to intersect the most prominent joint sets visible on the slope face.
For every discontinuity that intersected the line during scanline mapping, specific measurements were made, including water seepage, infill material, surface roughness, aperture, persistence, spacing, dip, and dip direction. Characterizing the rock mass fabric and determining the kinematic viability of different collapse modes required the use of these data. Additionally, the data assisted in the calculation of rock mass categorization metrics like GSI and RMR, offering a cross-check to core logging observations from the field. The sample of data sets is presented in Figures 4- 6 below.

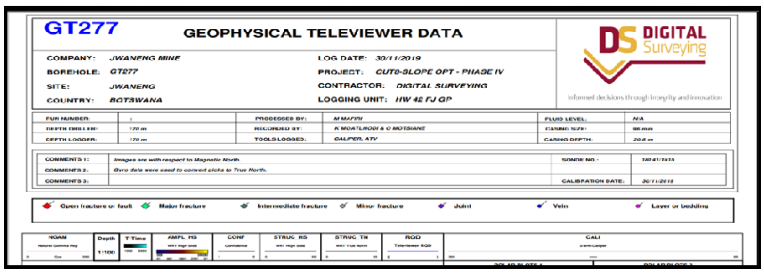

Fig. 4: Geophysical Data of Hole GT277, Televiewer Data Showing the Key to Indicate Different Labeling as Shown on Televiewer.

	73.69	296.08	17.47		LAY
	73.94	338.78	87.35		MAJ
	74.06	164.43	80.67		JOI
	74.89	158.82	89.86		JOI
	75.03	339.59	85.79		JOI

Fig. 5: Yellow Marking Showing Bedding, Major Structure, and Joint at Different Depths and Their Respective Angles About the True North (Far Right Recording).

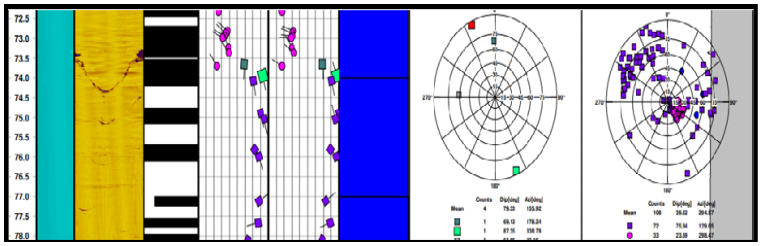

Fig. 6: For the Televiewer Analysis, One Line Stands for 10 Degrees. at 73.69 Depth, the Bedding Had an Angle of 17.47. This Helps in Knowing and Grouping Joint Sets Together and Understanding Their Orientations.

- Remote Sensing:

To acquire structural data in parts of the pit that were unsafe or unavailable for direct mapping, remote sensing techniques were used. Overlapping pictures of pit walls were taken by Unmanned Aerial Vehicles (UAVs) fitted with high-resolution cameras. To create 3D point clouds, digital surface models (DSMs), and orthophotos of the slope faces, these photos were processed using photogrammetry software.

6. Data processing

- Image Processing:

One tool used in mining for mapping, surveying, and tracking the movement of rock masses is 3D laser scanning technology. By using a transmitted and reflected laser beam to measure the distance of the reflected objects, the non-contact device gathers high-density data. Light detection and ranging (LiDAR) is the name given to this measurement and data recording technique. Millions of point cloud data are produced because of the scanning process, which displays the scan surface and discontinuity data like joint orientation, fracture density, and length. A rock face may be digitally scanned in three dimensions using laser scanner technology with a high resolution of up to millimeter accuracy (Fig.7).

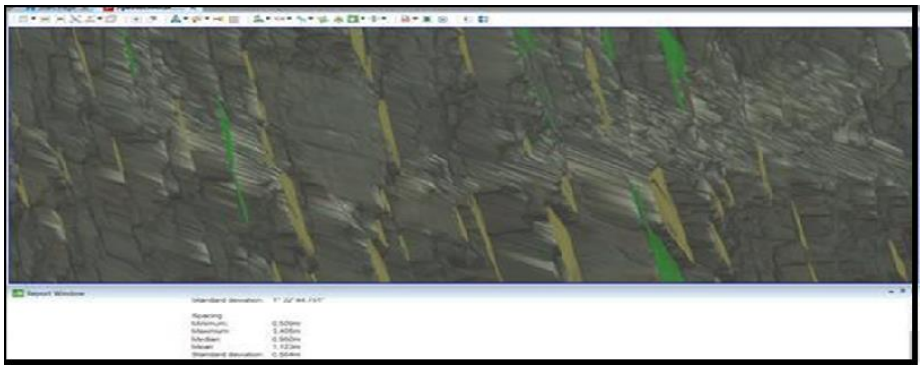

Fig. 7: All Structures Are Picked from Processed Laser Scans (Joints, Bedding, Faults) in Terms of Their Dip and Dip Orientations.

The other parameter measured from laser scans is Joint spacing and persistence. These can be measured automatically and manually from scans, and both methods will be used. It shows automatically measured parameters like the minimum length, maximum length, median, mean, and standard deviation. All parameters can be relatable when measuring manually on Maptek or onsite.

The assessment of rockfall and joint failure hazards in open-pit mines is the main topic of this literature review, which focuses on the geological and geotechnical conditions found in the Cut 8 South portion of Jwaneng Mine in Botswana. Due to the presence of intersecting joint sets, diverse lithology, and high bench heights, slope stability is still a major concern at Jwaneng Mine, one of the world's deepest and most structurally complicated diamond mines. The likelihood of structural failures has increased due to the mine's growing depth, making a thorough understanding of the failure mechanisms related to joints and other discontinuities essential.

- Rock Mass Properties:

Most of the rock mass at Jwaneng Mine falls into the fair to good category. The enormous Quartzitic Shale forms the foundation of the slope. The carbonaceous shales are fissile and graphitic on the main contacts, but the laminated shale has thin bedding. A description of the rock mass and deformation characteristics for the rock units of Cut 8's south-east wall slopes may be found in Table 2 (A & B) below.

Table 2: A) Summary of Rock Mass Properties

Code	Density Kg/M^3	Characterization				Strength					
		UCS (Mpa)	RMR	GSI	mi	Deep Rock Mass (>50m)			Shallow Rock Mass (<50m)		
						C(kPa)	(o)	σ_1	C(kPa)	(o)	σ_1
CS	2616	115	54	47	4.9	654	32	-173	354	37	-148
DM		214	66	54	12.6	1467	50	-357	903	54	-315
DOL	2880	222	61	49	8.9	1168	44	-346	694	48	-301
KIM		36	55	50	9	437	30	-46	174	36	-3.9
LS	2615	56	44	39	3.3	296	20	-118	130	23	-98
QS	2742	173	60	47	52	864	38	-350	508	40	-302

Table 3: B) Summary of Rock Mass Properties

Code	Deformation				
	MR	Ei (GPa)	ERM (GPa)		v
			Deep	Shallow	
CS	310	28	2.3	1.7	0.25
DM	431	96	12.7	9.2	0.24
DOL	325	76	7.8	5.7	0.25
KIM	273	10	1	0.7	0.25
LS	446	39	2.1	1.6	0.26
QS	350	61	5.3	3.9	0.26

- Joint Strength Properties:

Rocks can be heterogeneous and anisotropic due to the presence of structural discontinuities like joints, faults, or shear planes. For a slope design to be effective, joint strength qualities are crucial. Shear strength tests were performed on 55 samples with open joints and 49 samples with closed joints. The effective strength parameters were determined using the [7] formula.

$$\tau = \sigma_n \tan(\varphi_b + \mathrm{JRC} \log 10 (^{\mathrm{JCS}}/_{\sigma_n}))$$

Where:
JCS = Joint Compressive Strength (MPa)
JRC = Joint Roughness Coefficient
σ_n = Normal stress (MPa)

For foliation, discontinuities are often welded, while for subvertical connections, they are typically open joints. The surfaces of the joints range from new to somewhat worn. They are dry and have a straight, large-scale joint expression. Because of the displacements brought about by the extreme tectonic activity, the small-scale joint expressions range from smooth planar to slicken-sided undulating. Although the joint surfaces are usually clean, there may occasionally be calcite infilling in some areas. An analogous JRC number has been determined using these joint surface descriptors.

The Barlon-Bandis strength curve is used to calculate the Mohr-Coulomb strength parameters. By estimating the probable load on failure surfaces, the maximum shear strength was determined. An accurate approximation is provided by the lithostatic load. Regarding the slopes of Jwaneng. It has been determined to be 2MPa for deep rock mass and 0.5MPa for shallow failure planes that occur within 50m into the slope. Table 3 summarizes the shear strength of the joints in the south-east slopes of Jwaneng Cut 8.

Table 3: Summary of Joint Strength Peak Values for Cut 8 Foliation Discontinuities

Code	Strength							
	Foliation				Open Joints			
	d(kPa)	(o)	d(kPa)	(o)	D(kPa)	(o)	D(kPa)	(o)
CS	80.8	34	21	35	20.2	34	5.3	35
DM					25	34	6.7	36
DOL					22	37	5.7	38
KM					20	33	5.1	34
LS	80.3	34	20.9	35	20.1	34	5.2	35
QS	84.6	36	22.1	37	21.1	36	5.5	37

- Evaluation of Hydrogeological Components

The various hydro stratigraphic units that are present at Jwaneng Mine can be summarized as follows:

Kalahari Sands: The Kalahari sands occur entirely above the water table in the vicinity of Cut 8.

Shale Sequence (LS, CS, and QS): The top 200–250 meters of the shale strata exhibit variable fracturing, according to drilling results. The fissures are "pumpable" and transfer groundwater. The porosity of the shales is extremely low, 0.1% or less. The slime dams and "district-scale" groundwater flow replenish the sequence at shallow depths. It will be difficult to dissipate pore pressure if the upper portion of the unit is not pushed, since it will "feed" water into the slope. Nonetheless, it is demonstrated that pumping behind the crest significantly alters the slope's pressures. Unloading is predicted to result in a large pressure dissipation in the shale sequence if the recharge source outside the pit can be shut off by pumping.

Dolomites: According to the knowledge that is currently available, the dolomites are "compartmentalized" by the several high-angle fault zones in the region, even though they can be locally cracked and permeable. According to the information at hand, they do not seem to be related to the local groundwater flow system. Additionally, the porosity of the dolomites is limited (0.2–1.0%).

Kimberlites: Both the deeper contact between the kimberlite and the dolomite and the contact between the kimberlite and the shale exhibit fractures to differing degrees. The Kimberlites are more porous than the nearby country rocks, and when the fracture zones are drained, the

rock mass is probably going to display good depressurization. As seen in Figure 8, hydrogeological modelling conducted in 2009 indicates that the higher portions of the southeast wall are dry. The geotechnical feasibility assessment made this assumption.

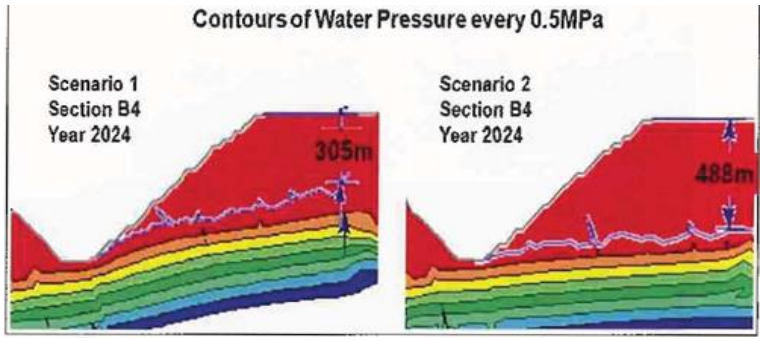

Fig. 8: Pore Pressures for the Cut 8 South East Slope (SRK Cut 8 Slope Design Review).

7. Results & discussion

To comprehend slope stability mechanisms, the core logging concentrated on locating and describing structural characteristics, especially bedding planes. Measurements of each observable discontinuity's dip, dip direction, structural type, and depth intervals were included in the core orientation data. Most of the logged structures were bedding planes, according to the core logging results, and they usually dipped at moderate degrees (32° to 50°) toward the south-southwest (dip directions ranged between 190° and 210°). The durability and continuity of these features throughout the rock mass were confirmed by the observation of these structures at different depths within the borehole. The orientation reliability was confirmed through top core marking, ensuring high confidence in the structural measurements (Fig.9).

	A	B	C	D	E	F	G	H	I	J	K	L	M	N	O	P	Q	R
1	x	y	z	Dip	Dip Direct	polarity	BH ID	DEPTH	Distance	DEPTH FR	DEPTH TO	INTERVAL	STRUCTUF	CLOSED	CORE MEA	LITH CODE	ORIENTAT	RQD %
2	-29443.6	-13322.8	996.0601	58	172	1	DD02	47.9	47.9	47.81	50.81	3	Bedding	FALSE	Top	QS	Top	66.67
3	-29443.7	-13322.8	995.9321	50	154	1	DD02	48.03	48.03	47.81	50.81	3	Bedding	FALSE	Top	QS	Top	66.67
4	-29443.7	-13322.7	995.5188	64	267	1	DD02	48.45	48.45	47.81	50.81	3	Joint	FALSE	Top	QS	Top	66.67
5	-29443.7	-13322.7	995.2136	50	154	1	DD02	48.76	48.76	47.81	50.81	3	Bedding	FALSE	Top	QS	Top	66.67
6	-29443.8	-13322.6	994.9183	48	183	1	DD02	49.06	49.06	47.81	50.81	3	Bedding	FALSE	Top	QS	Top	66.67
7	-29443.8	-13322.5	994.3079	50	166	1	DD02	49.68	49.68	47.81	50.81	3	Bedding	FALSE	Top	QS	Top	66.67
8	-29443.9	-13322.5	993.9141	50	166	1	DD02	50.08	50.08	47.81	50.81	3	Bedding	FALSE	Top	QS	Top	66.67
9	-29443.9	-13322.4	993.6482	66	293	1	DD02	50.35	50.35	47.81	50.81	3	Joint	FALSE	Top	QS	Top	66.67
10	-29443.9	-13322.4	993.3528	48	179	1	DD02	50.65	50.65	47.81	50.81	3	Bedding	FALSE	Top	QS	Top	66.67

Fig. 9: Oriented Discontinuity Input Data.

- Kinematic Analysis of Slope Failure Criteria

a) Direct Toppling

A kinematic analysis was performed using the DIPS software [8] to evaluate the potential for direct toppling failure in the Cut 8 South slope of Jwaneng Mine. This analysis is based on the orientation data obtained from field discontinuity mapping and core logging.

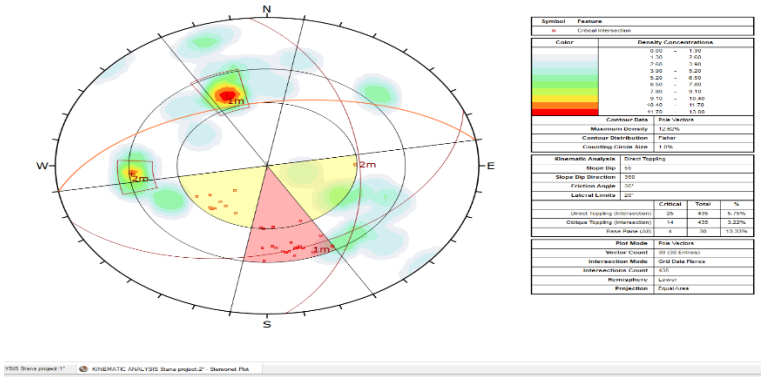

Fig. 10: Direct Toppling Analysis.

The parameters used in the analysis are typical of slope stability assessments in hard rock mines [9] & [10] :

- Slope Dip: 55°
- Slope Dip Direction: 350° (NNW)
- Friction Angle: 35°
- Lateral Limits: 20°
- Projection: Lower hemisphere, equal area stereo net
- Intersection Mode: Grid data planes

These inputs simulate realistic slope geometry and joint properties based on site-specific field observations and regional Geomechanical characteristics (Fig.10).

- Result Interpretation

Pole vectors of discontinuities are placed on density contours in the stereo net plot. Critical crossings where structural orientations permit possible immediate toppling are indicated by red-shaded areas.

Important conclusions include:

- Maximum Pole Density: 12.62%, indicating a concentration of planes with consistent orientation.
- Critical Intersections (Direct Toppling): 25 out of 435 (5.75%)
- Oblique Toppling Intersections: 14 out of 435 (3.22%)
- Total Toppling Susceptibility: Approximately 9.0%
- Base Plane Intersections: 4 (0.92%), implying a minimal risk of basal failure under toppling conditions.

According to these statistics, a significant minority of discontinuities satisfy the geometrical requirements for toppling, although the bulk of structural data do not. These meet with the slope face at angles smaller than the slope dip and greater than the friction angle, which is compatible with direct toppling failure mechanisms, especially where the discontinuities dip steeply into the rock mass [11].

Given that these conditions are satisfied in approximately 6% of the data, with additional oblique toppling risks, there is a moderate probability of localized toppling failures along the Cut 8 South wall.

b) Wedge Failure

- Kinematic Analysis

The type of kinematic analysis is Wedge Sliding, and its inputs are as follows

Slope Dip: 55

Slope Dip Direction: 350°

Type: Kinematic Analysis Type: Wedge Sliding

Maximum Density: 12.62%

Critical Intersections: Current (marked with red squares)

1m and 2m Wedges Analyzed

- Critical Intersections

Critical intersections, or where the large circles representing planes intersect the slope face, are marked by the red squares on the stereo net. The density of poles, or the likelihood of failure at such intersections, is represented by the intensity of the colour of the lines around these intersections. The maximum density is 12.62% (Fig.11).

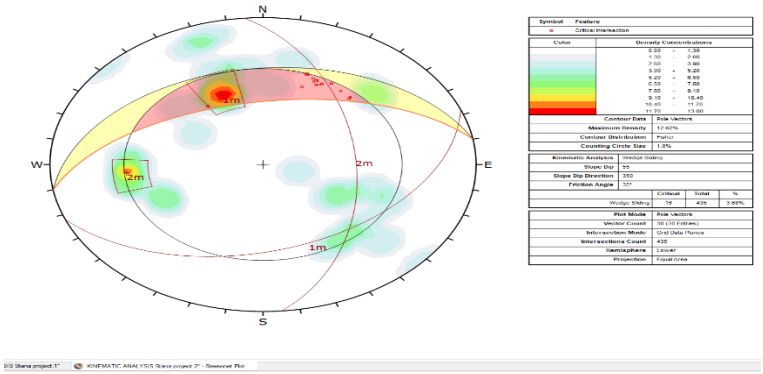

Fig. 11: Wedge Failure Criteria.

- Results Interpretation

Density of Poles: The probability of failure is ascertained by analyzing the poles' concentration around such crossings. The higher the density, the higher the probability of instability. The maximum density corresponding to possible failure surface concentration is 12.62%. The "1m" and "2m" wedges are analyzed by the study in terms of stability, considering orientation and the poles' closeness to their critical intersections.

c) Planar Failure

Pole directions of discontinuities in a rock mass are represented in the stereo net graph. The parameters of importance to kinematic analysis, which analyses the likelihood of slope failure, are presented in the tabulated data next to it. The region around a north-northeast trending and steep dip has the densest concentration of poles (12.62%). The stereo net graph has three major groups with the names "1m", "2m", and another "1m". The graphic also plots large circles by means of planar sliding analysis (Fig.12).

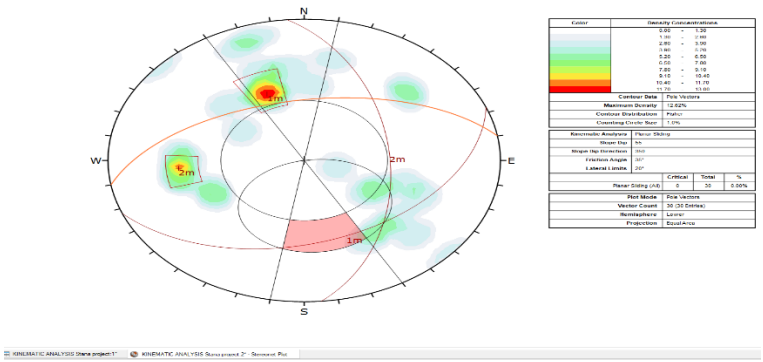

Fig. 12: Planar Failure Criteria.

- Kinematic Analysis Parameters

Key parameters from the table are:

- Slope Dip: 55°
- Slope Dip Direction: 350° (North-Northwest)
- Friction Angle: 35°

- Lateral Limits: 20°

These parameters define the potential failure plane (slope face) and the resistance to sliding (friction angle).

d) Planar Sliding Analysis Interpretation

The table indicates that for "Planar Sliding," there are 0 out of a possible 30 vectors in a state of criticality. Therefore, according to the supplied slope and discontinuity data, no planar sliding failure is anticipated using the given slope orientation and angle of friction. The distribution of contours, as Fisher means it is assumed the data approximate a Fisher distribution used in geological interpretation when dealing with direction data.

The stereo net diagram displays clustered orientations of discontinuities with a maximum intensity of 12.62%. Kinematic calculation assumes a slope dip of 55° and a dip direction of 350°. No plane sliding type failures are expected (0 out of 30 vectors are on the failure envelope).

- Slope Stability Representation

A jointed rock slope under surface loading was modelled in this research. The model was constructed and analyzed by using the software RS2. The heterogeneous geological unit, multiple joint networks, and boundary stress conditions are all part of the model. The purpose is to assess the slope performance and failure modes due to extra stress caused by structures on the surface or surcharges.

- Model Description
- Geometry and Materials

The modelled slope has a stepped profile and consists of two distinct lithological units:

- Dolomite (upper section),
- QS (Quartzite or Sandstone-like unit) (lower section).

The geometry has been discretized to have a high-resolution triangular mesh and has distinct material boundaries.

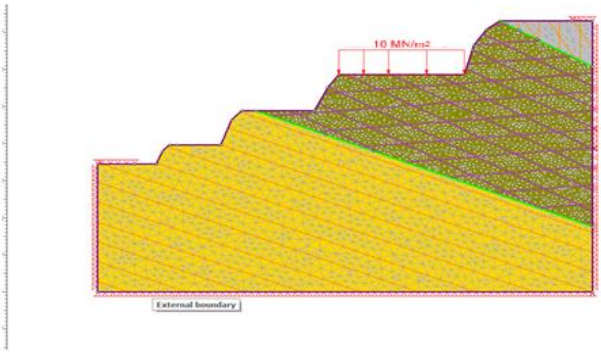

Fig. 13: Slope Representation with Different Lithologies from QS to CS to Dolomite.

- Analysis Approach

The model is prepared for finite element analysis with joint elements activated. The analysis considers:

- Shear Strength,
- Total displacement,
- Volumetric Strain.

This analysis was conducted with changing Stress reduction factor from 2 to 5 to 10 and a factor of safety of 1.5 for long-term.

A uniform weight distribution of 10 MN/m² is applied to the ramp (as shown in Fig.13) to account for the high activity area due to the movement of vehicles and machinery.

- Displacement Analysis

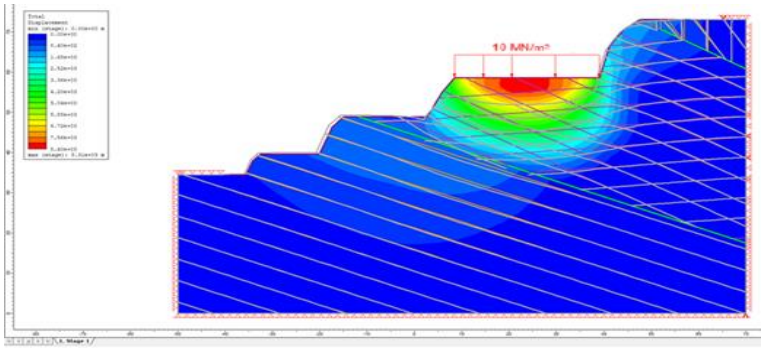

Fig. 14: Displacement Analysis.

- Displacement Contours

The figure shows the overall displacement contours in meters from RS2 after two locations at the slope crest were subjected to a 10 MN/m² surface load (Fig.14). A jointed rock slope's mechanical reaction to this severe loading is simulated by the model.

On the left, the displacement scale goes from:

Minimum:(Blue),0.00m

Max:(Red)8.31x10³meters

Although it aids in the visual identification of deformation zones, this excessive scale—likely the result of unrealistic load input or a lack of normalization of stress units—should be read relatively.

Key Observations

- Peak Displacement Zone: A circular distribution of high deformation in red and orange, situated just beneath the applied force on the crest.
- Direction of Deformation: Although not visible, displacement vectors inferred from contours indicate outward and downward movement, which is characteristic of possible slope failure modes such as rotational slide or toppling.
- Joint Influence: By decreasing material continuity and stiffness, joint networks beneath the loaded area increase displacement and serve as failure facilitators.
- Particularly when oriented negatively regarding slope geometry, joint sets develop mechanical flaws that greatly increase displacement under stress [9].
- Stress Transmission Path: Displacement zones spread into the lower QS unit from below, suggesting that the deformation pattern is influenced by both joint connection and material behaviour.

Shear Strength Analysis

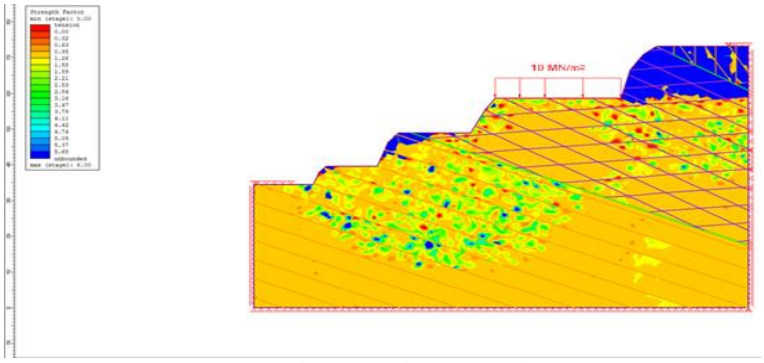

Fig. 15: Shear Strength Representation.

Contours and Grids:

- Various survey lines or portions throughout the area under analysis may be represented by the grid lines.
- To help geologists or engineers comprehend the spatial distribution of material strength, contours may show different strength components.

Strength Factor Visualization:

- A color-coded map showing the "Strength Factor" (Fig.15) for a certain area is displayed in the image. The colours vary from blue, which denotes greater strength, to red, which denotes less strength. The orange shows medium strength in most parts of the slope and blue in the upper most bench.
- In mining and civil engineering applications, the strength factor is typically employed to evaluate the stability of rock masses or soil.

Volumetric Strain Analysis

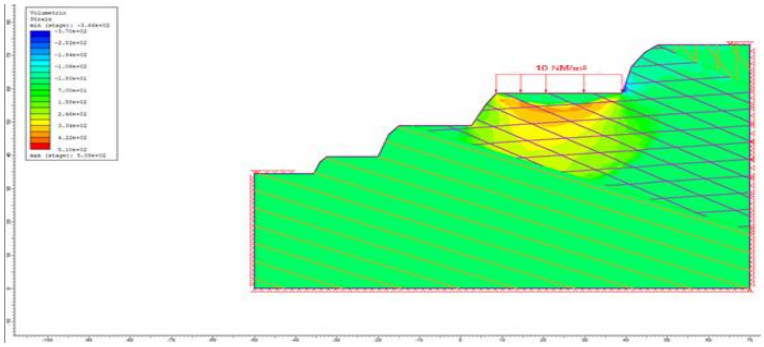

Fig. 16: Volumetric Strain Analysis.

Grid and Contour Representation:

- To associate certain strain values with geographic coordinates, the grid lines may serve as spatial divisions of the area being analyzed. For site-specific evaluations in engineering projects, this is crucial.

Volumetric Strain Visualization:

- From blue, which indicates compressive strain, to red, which indicates tensile strain, the colour gradient depicts various amounts of volumetric strain. This is essential to comprehending the deformation of materials under stress (Fig.16).
- Volumetric strain varies considerably throughout the examined region, with warmer colours denoting higher strain in the ram areas due to it being a high activity area.

8. Discussion

- Geological and Structural Characterization

The study draws attention to the Jwaneng Mine's complex geology, which includes intersecting discontinuities, steeply descending joint sets, and fluctuating rock mass conditions that all contribute to slope instability [6]. The mechanical behaviour of the rock mass is influenced by the considerable variability of the lithological succession, which includes dolomites, quarzitic shales, and kimberlite pipes. To evaluate possible collapse modes, core logging and scanline surveys identified persistent bedding planes that dipped considerably (32°–50°) toward the south-southwest [12] & [13].

- Kinematic Analysis of Slope Failure Modes

Direct Toppling: Where steeply dipping joints connect the slope face, about 9% of discontinuities satisfied the geometric requirements for toppling, suggesting localized instability [11]. This is consistent with findings in comparable hard rock settings.
Wedge Failure: In situations when joint densities were high (12.62% pole concentration), there was a considerable risk of two joint sets intersecting with a daylighting line of intersection. It is well known that wedge failures happen quickly, particularly on slopes that are structurally controlled [9].
Planar Failure: With the specified friction angle (35°) and slope geometry (55° dip, 350° dip direction), no critical planar sliding vectors were found. This implies that while planar failures are still a worry in other areas of the pit, they are less common in the section under study [14]

- Numerical Modelling and Slope Stability Assessment

Joint networks and lithological changes were incorporated into the RS2 finite element model, which approximated slope behaviour under surface loading. Among the important findings were:
Displacement Analysis: Under simulated stress (10,000 MN/m^2), high deformation zones were located close to the slope crest, suggesting possible rotational sliding or toppling [15]. Joint networks functioned as failure facilitators, amplifying displacement.
Shear Strength and Volumetric Strain: The upper dolomite unit was dominated by compressive strain, whereas the lower benches displayed weaker zones (red/orange) in the strength factor distribution. The necessity of targeted reinforcement in high-risk locations is highlighted by this heterogeneity [16].

9. Conclusion

- This study has determined the primary failure mechanisms and suggested practical

The study found that crossing joint sets and steeply dipping discontinuities are the main causes of wedge failure and direct toppling on the Cut 8 South slope. According to kinematic analysis with DIPS software, wedge failures were common in areas with high joint density, and about 9% of discontinuities satisfied the geometric requirements for toppling. Planar sliding, on the other hand, was thought to be less possible with the current slope configuration, while it is still a worry in other pit portions.
These findings were further supported by numerical modelling with RS2, which identified high-risk deformation zones close to the crest and simulated slope behaviour under surface loads. Displacement patterns were strongly impacted by the existence of persistent joint networks, highlighting the necessity of focused reinforcement techniques. By showcasing the benefits of interdisciplinary techniques in slope stability analysis, this study makes a substantial contribution to the field of geotechnical engineering in mining.
Probabilities of further rockfall or joint failure risks at the site (i.e., Jwaneng Pit) are very likely, as shown by the geotechnical and structural indicators. Higher joint frequency imparts more weakness in the rocks. Secondly, the more the number of joint intersections, the greater the chances of wedge failure.

10. Recommendation

Controlled methods that reduce the effects of vibration on joined rock masses should be used to optimize blasting operations. To restrict disturbance to important discontinuities, this entails lowering charge weights and meticulously sequencing bursts.
Measures for slope reinforcement are equally important. Essential structural support must be provided via the targeted placement of shotcrete, wire mesh, and rock bolts in high-risk areas. To guarantee cost-effective execution, these interventions should be ranked in order of importance using a thorough joint pattern analysis.
Another essential element is efficient water management. To regulate pore pressures, a thorough drainage system that includes dewatering wells and horizontal drains must be set up. As mining moves deeper, timely modifications will be possible thanks to routine groundwater level monitoring.

Acknowledgements

The authors express their sincere thanks to the Head, Department of Mineral Resources, and the Department of Mining. Botswana International University of Science & Technology. Our sincere thanks are due to the Debswana Jwaneng Mines, Botswana for allowing us to publish the research findings in the form of a research paper.

References

[1] Jaboyedoff, M., Hammouda, M. B. and Derron, M. H (2021) The Rockfall Failure Hazard Assessment: Understanding and Reducing Landslide Disaster Risk, K. Sassa et al. (eds.)‹ ICL Contribution to Landslide Disaster Risk Reduction, pp.55-83. https://doi.org/10.1007/978-3-030-60196-6_3.
[2] Xiaa, M., Lib, Hai, Jianga, N., Chenb, J. & Zhoua, J. (2022) Risk Assessment and Mitigation Evaluation for Rockfall Hazards at the Diversion Tunnel Inlet Slope of Jinchuan Hydropower Station by UsingThree-dimensional Terrestrial Scanning Technology, KSCE Journal of Civil Engineering (2023) , Vol.27(1), pp.181-197. https://doi.org/10.1007/s12205-022-1679-8.
[3] Du, J., Xiao, F., Chai, B., Yin, K., Juan Du, Xiao Feng, Bo Chai, Kunlong, Yin, K. & Li Z. (2025). Physically based deterministic rockfall hazard assessment integrating multi-failure modes at large scale: A case study of Tiefeng Township, Chongqing, China, Journal of Rock Mechanics and Geotechnical Engineering,pp.1-26. https://doi.org/10.1016/j.jrmge.2024.12.023.
[4] Viorel, I. (2009). Rockfall Hazard Assessment, Case study: Lotru Valley and Olt Gorge, Re vi s ta de geomor fologie – vol. 11, pp. 101-108. https://www.geomorfologie.ro/wp-content/uploads/2015/07/Revista-de-geomorfologie-nr.-11-2009-13.ilinca.pdf.
[5] Debswana.com. (2024). From https://www.debswana.com/jwaneng/.
[6] R.J. Brown, R.J., Gernon, T, Stiefenhofer, J. &. Field, M (2008).Geological constraints on the eruption of the Jwaneng Centre kimberlite pipe, Botswana, Journal of Volcanology and Geothermal Research, Volume 174, Issues 1–3, pp. 195-208, https://doi.org/10.1016/j.jvolgeores.2007.12.032.
[7] Barton - Bandis | Rock - Shear Resistance Criteria, Fine software, https://www.finesoftware.eu/help/geo5/en/barton-bandis-01/.
[8] RocScience. (2023). Stereo net and Kinematic Analysis Software. From DIPS: https://www.rocscience.com/.
[9] Hoek, E. and Bray, J.W. (1981) Rock Slope Engineering. Revised 3rd Edition, The Institution of Mining and Metallurgy, London, 341-351. https://www.scirp.org/reference/referencespapers?referenceid=1673353 . https://doi.org/10.1201/9781482267099.
[10] Wyllie, D.C. & Christopher, W. M. (2014). Rock Slope Engineering. Civil and Mining (4th ed.),456p.https://civilenglineering.wordpress.com/wp-content/uploads/2014/10/rock_slope_engineering_civil_and_mining.pdf.

[11] Goodman, R. E. (1980). Introduction to Rock Mechanics. John Wiley & Sons, New York, 289p. https://www.scribd.com/document/131171095/Goodman-R-E-Introduction-to-Rock-Mechanics-2nd-Edition.
[12] ISRM. (1978). International society for rock mechanics commission on standardization of laboratory and field tests: Suggested methods for the quantitative description of discontinuities in rock masses. International Journal of Rock Mechanics and Mining Sciences & Geomechanics Abstracts, pp.319–368. https://doi.org/10.1016/0148-9062(78)91472-9.
[13] Hoek, E. & Brown, E,T (1997). Practical estimates of rock mass strength. International Journal of Rock Mechanics and Mining Sciences, pp.1165–1186. https://doi.org/10.1016/S1365-1609(97)80069-X.
[14] Aamodt, M. T., Grimstad, G. & Nordal, S.(2025). Effects of strength anisotropy on the stability of slopes. In IOP Conference Series: Earth and Environmental Science. pp.1-11. https://iopscience.iop.org/article/10.1088/1755-1315/710/1/012025/pdf.
[15] Baczynski, N.R.P., Sheppard, I.K. ,Smith, K.J., Simbina, P., Sakail, R. (2008). Toppling Slope Failure—Predicted Versus Actual, SHIRMS 2008 – Y. Potvin, J. Carter, A. Dyskin, R. Jeffrey (eds) © 2008 Australian Centre for Geomechanics, Perth pp. 1-14, https://doi.org/10.36487/ACG_repo/808_10.
[16] Grenon, M & Hadjigeorgiou, J (2007). A design methodology for rock slopes susceptible to wedge failure using fracture system modelling. Engineering Geology, Volume 96, Issues 1–2, , pp. 78-93. https://doi.org/10.1016/j.enggeo.2007.10.002.